

# Structural and Biochemical Changes in Lungs of 3-Methylindole-Treated Rats

Leslie W. Woods, Dennis W. Wilson,  
Mary J. Schiedt, and Shri N. Giri

*From the Departments of Veterinary Pathology and  
Veterinary Pharmacology/Toxicology, School of Veterinary  
Medicine, University of California, Davis, California*

***Effects of a single dose of 3-methylindole (3-MI) (250 mg/kg intraperitoneally) were studied at different times ranging from 12 hours to 2 weeks post-treatment (PT). Microscopic study revealed mild Clara cell injury 24 hours PT and mucus hyperplasia 24 hours to 2 weeks PT. Diffuse type I alveolar epithelial cell necrosis occurred at 48 hours, followed by type II cell hyperplasia. Septal edema and accumulation of interstitial and capillary polymorphonuclear leukocytes and perivascular mixed mononuclear inflammatory cells accompanied the injury and repair. A gradual resolution of lesions with persistent mononuclear inflammatory cellular clusters at septal junctions, focal septal fibrosis, and accumulation of alveolar macrophages was evident at 1 and 2 weeks PT. Collagen, measured as hydroxyproline, in 3-MI-treated rats was significantly increased to 130% and 139% of control (3.0 mg/lung) at 1 and 2 weeks PT, respectively. Biphasic peaks of plasma 6-keto-prostaglandin  $F_{1\alpha}$  occurred at 12 to 24 hours and at 96 hours PT with 3-MI and thromboxane  $B_2$  was elevated 12, 48, and 96 hours PT. Right ventricular/left ventricular and septal weight was increased to 120% and 140% of the control 1 and 2 weeks PT. We concluded that 3-MI induces alveolar septal injury in the rat with relatively complete repair of the alveolar epithelium and residual mild focal septal fibrosis and pulmonary hypertension 2 weeks PT. Arachidonic acid-derived mediators and inflammation are associated with 3-MI-induced lung injury. (Am J Pathol 1993, 142:129-138)***

3-Methylindole (3-MI), a ruminal fermentation product of L-tryptophan, is thought to be the etiological

factor in acute bovine pulmonary edema and emphysema in cattle.<sup>1</sup> Evidence suggests that 3-MI is metabolized by the cytochrome P-450-dependent mixed-function oxidases in the lung to a reactive electrophilic intermediate that alkylates cellular macromolecules, resulting in pneumotoxicity.<sup>2</sup>

3-MI is pneumotoxic to cattle, sheep, goats, and mice. Lesions induced by 3-MI in these species include diffuse type I alveolar epithelial cell necrosis with subsequent type II cell hyperplasia, capillary endothelial cell necrosis, Clara cell necrosis, interalveolar septal edema and inflammation,<sup>3-9</sup> and changes in the pulmonary vascular wall.<sup>10,11</sup> In contrast, 3-MI induces bronchiolitis and obstructive pulmonary disease in horses with apparently no alveolar epithelial cell injury.<sup>12</sup> Two previous studies have evaluated 3-MI-induced lung injury in rats.<sup>13,14</sup> In one study, light microscopic changes in the lungs of rats after intraperitoneal injection with 3-MI included Clara cell necrosis, endothelial cell necrosis in pulmonary veins and venules, and type II cell proliferation.<sup>13</sup> A second study using electron microscopy described Clara cell necrosis in the absence of endothelial cell or type I epithelial cell changes in rats 24 hours after administration of 3-MI.<sup>14</sup> A complete time-course study of light microscopic and ultrastructural changes induced by 3-MI has not been performed in the rat.

The role of inflammation in 3-MI toxicity has not been evaluated in the rat. Arachidonic acid is a constituent of cell membrane phospholipids of a wide variety of cell types. Arachidonic acid is metabolized via the cyclo-oxygenase pathway to prostaglandins and thromboxanes. Elevated plasma levels of thromboxane  $A_2$  ( $TxA_2$ ) and prostaglandins have been demonstrated in many pulmonary diseases including adult respiratory distress syndrome, bleomycin-induced pulmonary fibrosis, and cystic fibrosis.<sup>15-17</sup> Thromboxane  $B_2$  ( $TxB_2$ ) is a stable metabolite of

---

Supported in part by National Heart Lung and Blood Institute grant 2R01HL27354 and National Institutes of Health grant ESO 3343.

Accepted for publication June 25, 1992.

Address reprint requests to Dr. Dennis W. Wilson, Department of Veterinary Pathology, School of Veterinary Medicine, University of California, Davis, CA 95616.

TxA<sub>2</sub> that is a potent vasoconstrictor and platelet-aggregating agent. Thromboxanes are produced primarily by platelets and neutrophils (during phagocytosis). Endothelial cells and resident lung cells, including lung fibroblasts, also have been shown to synthesize TxA<sub>2</sub>.<sup>18,19</sup> Plasma 6-keto-prostaglandin F<sub>1α</sub>, a stable metabolite of prostaglandin I<sub>2</sub> (PGI<sub>2</sub>), is a vasodilator and inhibits inflammation-induced platelet aggregation. It is synthesized primarily by endothelial cells, but type II alveolar epithelial cells, alveolar macrophages, and lung fibroblasts also have been shown to produce PGI<sub>2</sub>.<sup>20-22</sup>

The purpose of this study was to demonstrate time-related light and electron microscopic changes induced in rats following a single, intraperitoneal dose of 3-MI and compare these changes with those induced in previous studies in the rat. Additional objectives were to correlate time-related pathologic changes with circulating levels of the inflammatory mediators TxA<sub>2</sub> (measured as TxB<sub>2</sub>) and PGI<sub>2</sub> (measured as 6-keto-PGF<sub>1α</sub>), and to determine whether injury induced by 3-MI is reversible or irreversible by evaluating collagen deposition (fibrosis) and right ventricular hypertrophy as an indication of pulmonary hypertension.

### Materials and Methods

Adult Sprague-Dawley rats (Bantin and Kingman, Fremont, CA), 300 to 350 g, were housed two per cage and fed rat pellets and water *ad libitum*. After a 7-day acclimation period, 63 rats were given a single, intraperitoneal injection of a 12.5% (w/v) solution of 3-MI in propylene glycol (250 mg/kg). Twenty-one rats served as controls and were injected with pro-

pylene glycol intraperitoneally. Twelve rats (three controls and nine treated rats) were killed at each time interval of 12, 24, 48, 72, and 96 hours, 1 week, and 2 weeks post-treatment (PT) by exsanguination under pentobarbital anesthesia.

### TxB<sub>2</sub> and 6-Keto-PGF<sub>1α</sub>

Blood levels of TxB<sub>2</sub> and 6-keto-PGF<sub>1α</sub> were measured by radioimmunoassay (RIA) according to the procedure described by Chandler and Giri.<sup>16</sup> Whole blood was collected in heparinized syringes, transferred to tubes containing 2 mg of indomethacin, mixed, and centrifuged. The resulting plasma was measured, acidified by 6 N HCl (0.1 ml/ml of plasma), and spiked with approximately 2000 cpm [<sup>3</sup>H]-TxB<sub>2</sub> or [<sup>3</sup>H]-6-keto-PGF<sub>1α</sub> to monitor recoveries of both TxB<sub>2</sub> and 6-keto-PGF<sub>1α</sub>. Plasma samples were frozen at -20 C until assayed. Plasma samples for prostaglandin or TxB<sub>2</sub> measurement were extracted with chloroform in the presence of NaCl. The chloroform extract was dried and reconstituted in 0.1 mol/L (molar) phosphate-buffered saline with 0.1% gelatin. Predetermined aliquots of reconstituted sample were used in the RIAs for TxB<sub>2</sub> and 6-keto-PGF<sub>1α</sub>. After overnight incubation, bound counts were separated from unbound counts using ice-cold dextran-coated charcoal in the phosphate-buffered saline and gelatin. Levels of prostanoids were calculated from RIA standard curves. A 300- to 400-μl aliquot from each sample was used to determine percent recovery. Control values represent an average of values obtained from three propylene glycol-treated animals at each time point. Values were averaged into one control value because there were no radical differences in control values between time points.

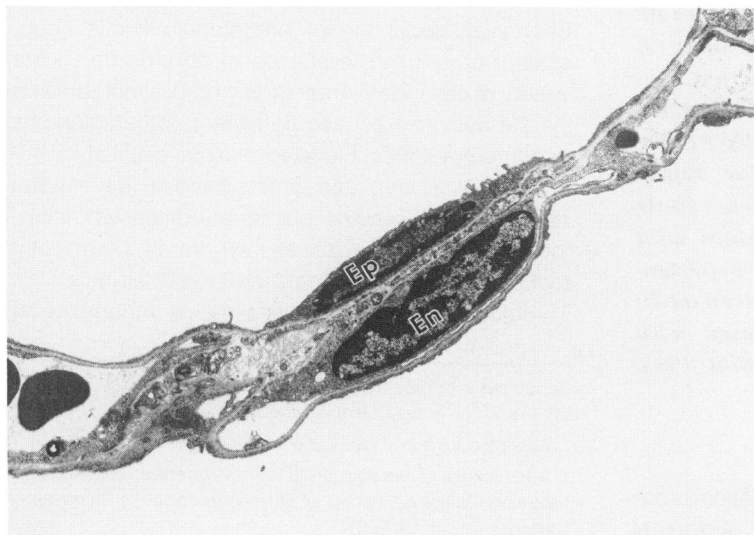
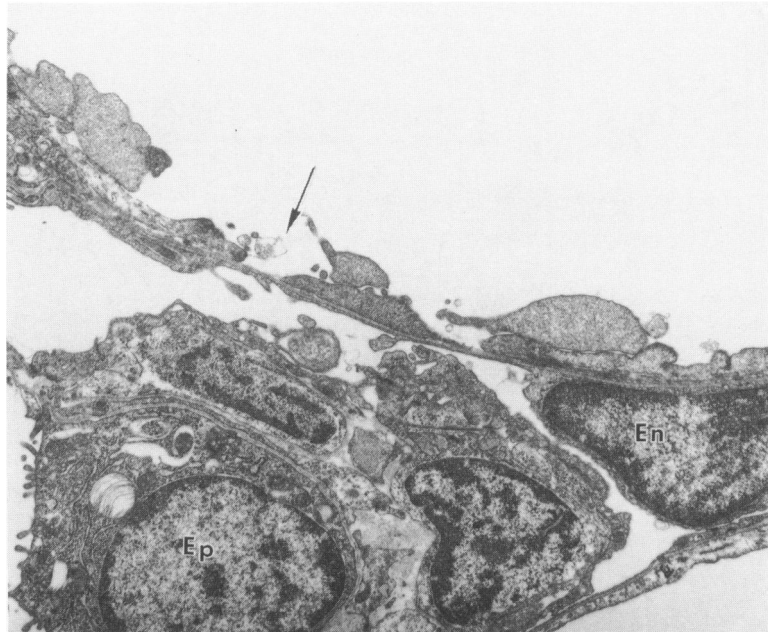


Figure 1. Transmission electron photomicrograph of the interalveolar septal wall of a control rat. A type I epithelial cell (Ep) and an endothelial cell (En) are shown. (Uranyl acetate and lead citrate, ×3120.)



**Figure 2.** Transmission electron photomicrograph of the interalveolar septal wall of a rat 48 hours PT with 3-MI. There is type I cell necrosis with exposure of the basal lamina (arrow). Note the absence of endothelial (En) and type II epithelial (Ep) cell injury. (Uranyl acetate and lead citrate,  $\times 5345$ .)

### Light and Electron Microscopy

At each time point, three 3-MI-treated rats and one control rat were randomly chosen for histological studies. The tracheas and right ventricles were cannulated and the lungs were fixed by tracheal and vascular perfusion at constant pressures of 20 cm H<sub>2</sub>O and 100 cm H<sub>2</sub>O, respectively, with modified Karnovsky's fixative (550 mOsm, pH 7.4).<sup>23</sup> Four 1 × 5 × 5 mm tissue blocks of select airway generations

(generations 5, 6, 8, and 9) off the intrapulmonary bronchus of the left lobe were taken from each rat according to the procedure previously described by Wilson and associates<sup>24</sup> and were embedded in epon arylidite. A 1- $\mu$ m section from each of the four tissue blocks was stained with toluidine blue and examined by light microscopy. Two thin sections, one that included the central airways and another with the surrounding parenchyma, were cut from the tissue block with generation 6 and mounted on grids,

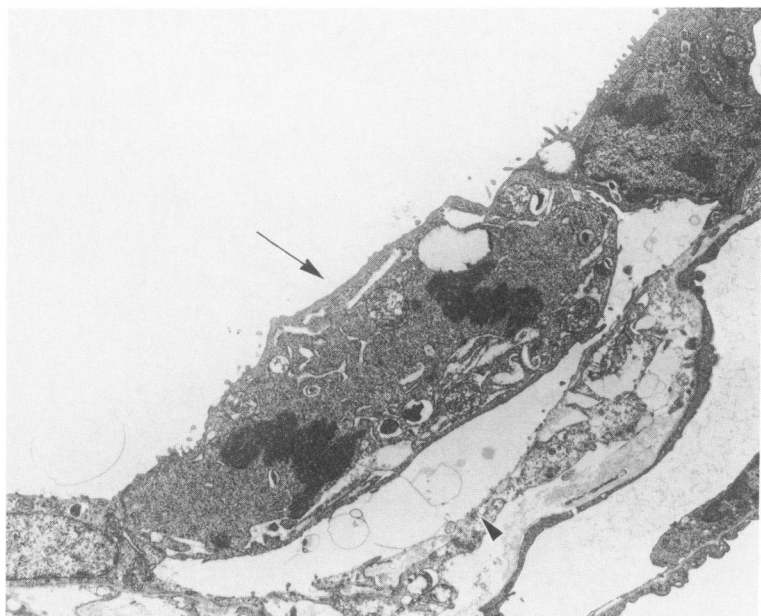


**Figure 3.** Transmission electron photomicrograph of the interalveolar septal wall of a rat 96 hours PT with 3-MI. Type II epithelial cell hyperplasia is demonstrated by type II cell in mitosis (arrow) adjacent to another type II cell. The mitotic type II cell appears to have separated from the disrupted basal lamina (arrowhead). There is electron lucency (edema) of the interstitium. (Uranyl acetate and lead citrate,  $\times 5037$ .)

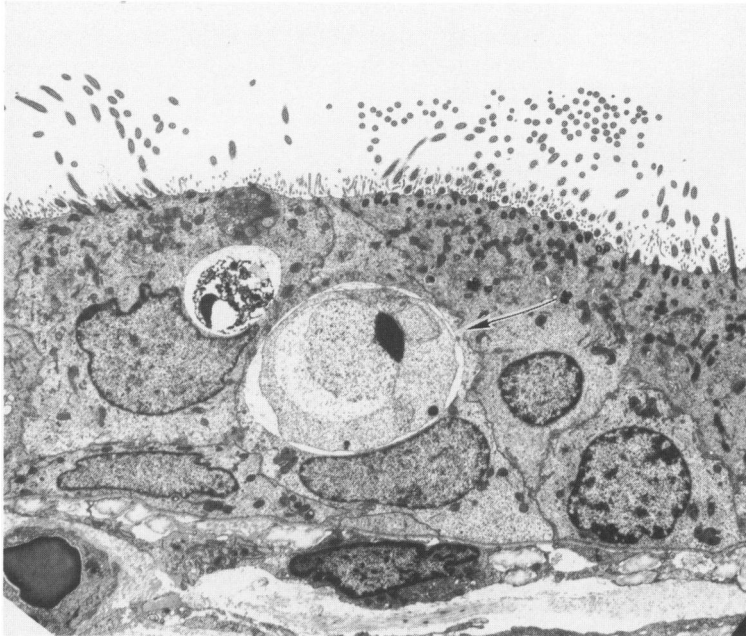


**Figure 4.** Transmission electron photomicrograph of bronchiolar epithelium from rat 48 hours PT with 3-MI. Clara cell contains large autolysosomal vacuole (arrow). Adjacent ciliated epithelial cell contains a small autolysosomal vacuole, which was a rare finding. (Uranyl acetate and lead citrate.  $\times 3,333$ .)

stained with uranyl acetate and lead citrate, and examined with a Zeiss 10A transmission electron microscope.

### *Vessel Measurements*

Measurements of a cross-sectional area of pulmonary arteriolar adventitia, media, and lumina were done with computer-assisted planimetry (JAVA, Jandel Scientific, Corte Madera, CA). Eight cross-sectional profiles of parenchymal (intra-acinar) arterioles per block were selected. Vessels were identified as arterioles on the basis of location near alveolar duct structures and previously published histologic criteria.<sup>24</sup> Measurements of the entire cross-sectional area at the border of the adventitia with alveolar parenchyma, area internal to the external elastic lamina, and lumen area were made. The percentage of total cross-sectional area represented by adventitia, media, and lumen was calculated by subtracting

the area of the lumen from the total area. The percentage of total cross-sectional area represented by adventitia, media, and lumen was calculated by subtracting

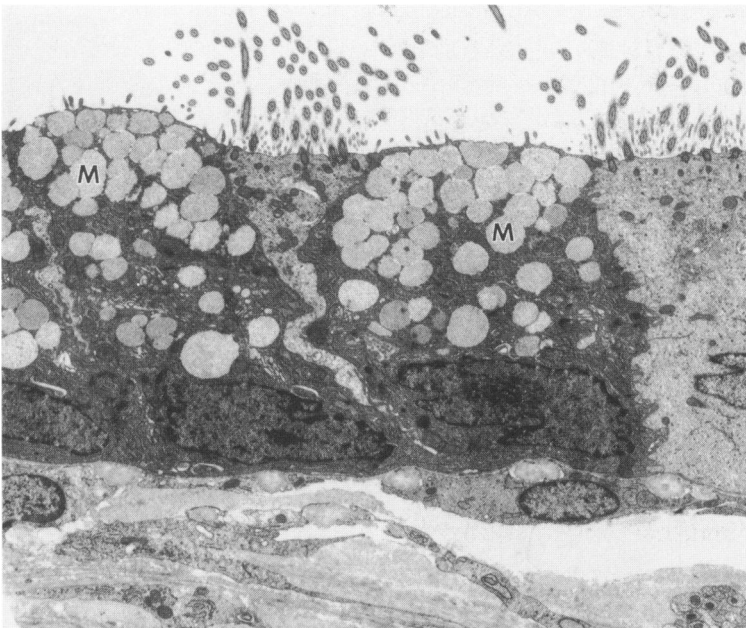


**Figure 5.** Transmission electron photomicrograph of bronchiolar epithelium from rat 96 hours PT with 3-MI. Mucus "metaplasia" of Clara cells. Note mucus granules (M) in the apical cytoplasm of Clara cells. Mucus cells were not present in the bronchioles of control rats. (Uranyl acetate and lead citrate.  $\times 4,380$ .)

tion of the other components of these measurements and expressed as percent of total area. Average arteriolar external and lumen diameters were estimated by calculating the diameter of a true circle with that area.

### *Collagen Deposition and Ventricular Septal Weights*

The lung lobes were excised at the hili and immersed in liquid nitrogen. The lung tissue samples were stored at  $-80^{\circ}\text{C}$  until assayed for collagen. Hearts were dissected from the lung tissue. Atria and large vessels were removed and the right ventricular wall was cut flush with the septum and weighed. The left ventricle was weighed and the right ventricular wall (RV) to left ventricular wall + septum (LV + S) was calculated. One-milliliter aliquots of whole lung homogenates in saline were used to determine total lung collagen in rats 1 and 2 weeks PT, according to the procedure previously described.<sup>25</sup> Samples were precipitated with ice-cold trichloroacetic acid and precipitates were hydrolyzed overnight in Teflon-sealed capped tubes in 2 ml of 6 N HCl. The hydrolysates were spiked with [ $^3\text{H}$ ]hydroxyproline and decolorized with charcoal. The spiked samples were filtered and neutralized, and the volumes were recorded. An aliquot of each was counted for recovery, and duplicate aliquots were used for the assay. The color was developed with *p*-dimethylaminobenzaldehyde after timed oxidation using chloramine-T. Each value was corrected for recovery.

### *Statistics*

Statistical analysis was done with a microcomputer-based statistical analysis program (Numbercruncher statistical systems, version 5.0, Kaysville, UT). Treatment effects on ventricular weight ratios, pressures, and vessel measurements were evaluated by analysis of variance with Fischer's least significant difference post-hoc test. Differences between individual group means were compared by *t*-test. Nonparametric evaluation of subjective light microscopic lesion scores was done by comparison of individual group means by the Mann-Whitney *U*-test.

### *Results*

Light and ultrastructural changes were not detected 12 hours PT with 3-MI. Alveolar septal changes were minimal 24 hours PT and limited to sporadic mitochondrial swelling in type I epithelial cells. There was

a broad spectrum of ultrastructural changes in 80% to 90% of type I cells 48 hours PT compared with control rat lungs (Figure 1), which included cytoplasmic blebbing and swelling of smooth endoplasmic reticulum and, less frequently, overt necrosis and denudation of the alveolar septal basal laminae (Figure 2). Type I epithelial cell necrosis was most severe 72 and 96 hours PT and resolved 1 week PT. Type II epithelial cells were hypertrophic and mildly hyperplastic 48 hours PT. Type II cell hyperplasia was marked 72 hours PT, maximal 96 hours PT (Figure 3), and resolved 2 weeks after 3-MI treatment. There was no morphologic evidence of endothelial or type II epithelial injury (Figure 2) except for rare focal necrosis associated with local aggregates of neutrophils. Airway changes were seen primarily in Clara cells 24 hours PT and characterized by loss of secretory granules, prominent smooth endoplasmic reticulum, and formation of autolysosomes (Figure 4). Mucus goblet cells were present in bronchioles 48 hours–2 weeks PT (Figure 5) but were not present in the bronchioles of any of the control rats (Figure 6).

Interstitial edema was first evident 24 hours PT with 3-MI when compared with lungs from control rats (Figure 7). Forty-eight through 96 hours PT, there was diffuse accumulation of mixed inflammatory cell infiltrates (Figure 8), composed predominantly of neutrophils, monocytes, and macrophages in the interalveolar capillaries and septa. Alveolar macrophages were diffusely scattered throughout the parenchyma within alveolar spaces 72 and 96 hours PT. Interstitial infiltrates persisted as mononuclear inflammatory cell clusters associated with focal fibrosis at septal junctions and around intrapulmonary vessels 1 week PT (Figure 9) and was diminished, but still apparent, 2 weeks PT (Figure 10). A mild, diffuse thickening of the interalveolar septal interstitium, which was not apparent on examination using light microscopy, was evident ultrastructurally 1 and 2 weeks postinoculation and associated with an increase of interstitial collagen.

Intra-acinar pulmonary vessels displayed mild intimal and medial electron lucency (edema) 48 hours PT, which progressed to a moderate perivascular edema with adventitial mononuclear inflammatory cell infiltrates 72 and 96 hours PT. The adventitia and tunica media of alveolar duct-associated intra-acinar pulmonary vessels showed significant thickening 1 week PT (Figure 11) with return to control levels 2 weeks PT (Table 1). Adventitial thickening was due to edema and mononuclear inflammatory cell infiltrates, and medial thickening was due to a mild, diffuse increase in the extracellular matrix and smooth muscle hyperplasia.

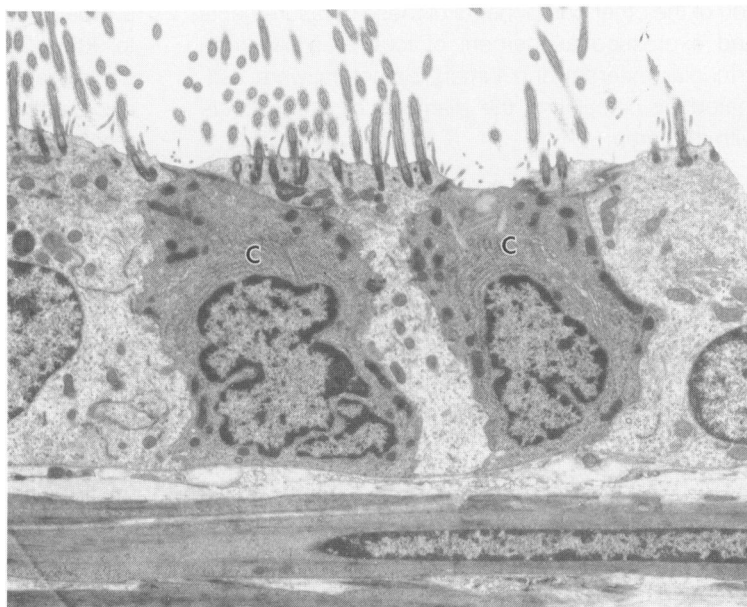


**Figure 6.** Electron photomicrograph of bronchiolar epithelium from control rat. Two Clara cells (C) are located between ciliated epithelial cells. (Uranyl acetate and lead citrate,  $\times 5030$ .)

Plasma levels of 6-keto-PGF<sub>1 $\alpha$</sub>  in 3-MI-treated rats were biphasic and significantly elevated compared with controls 12 to 24 hours and 96 hours PT (Figure 12). TxB<sub>2</sub> was significantly elevated 12, 48, and 96 hours PT when compared with controls (Figure 13). Collagen (measured as hydroxyproline) showed a significant increase of 130% and 139% of controls (3 mg/lung) at 1 and 2 weeks PT with 3-MI. RV/LV + S was increased to 120% and 140% of the control at 1 and 2 weeks PT (Figure 14).

### Discussion

It appears there is wide species variation in response to a single dose of 3-MI with respect to effective dose, response time, and target cell population. Our

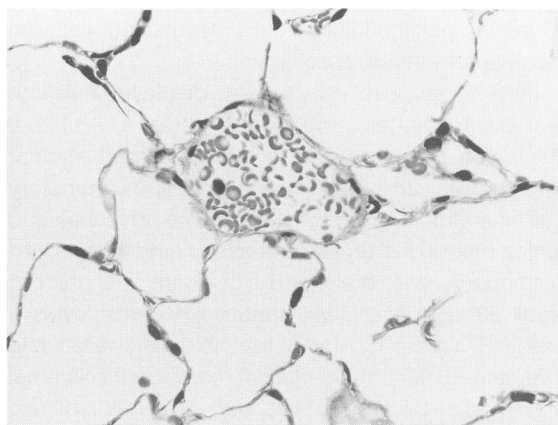


**Figure 7.** Light photomicrograph of lung from control rat. (Toluidine blue,  $\times 650$ .)

study demonstrates that the time interval between the administration of 3-MI and ultrastructural changes is much longer in the rat than reported for ruminants. 3-Methylindole administered to goats (40 mg/kg) induces changes similar to those described in the rats in this study, which are evident 30 minutes after treatment and become progressively more severe by 24 hours PT.<sup>7</sup> Unless there are early changes that are transient and completely resolved by 12 hours PT, it appears the response time from inoculation to morphologic evidence of injury in the rat is delayed and may be attributed to alternate metabolic pathways in this species.<sup>2</sup>

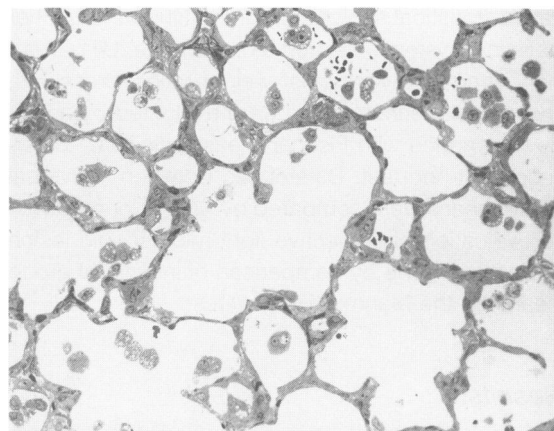


**Figure 8.** Light photomicrograph of lung from a rat 96 hours PT with 3-MI. There is thickening of the interalveolar septa with type II epithelial cell hyperplasia and accumulation of inflammatory cells in the interstitium. Large numbers of alveolar macrophages have accumulated in alveoli. (Toluidine blue,  $\times 400$ .)

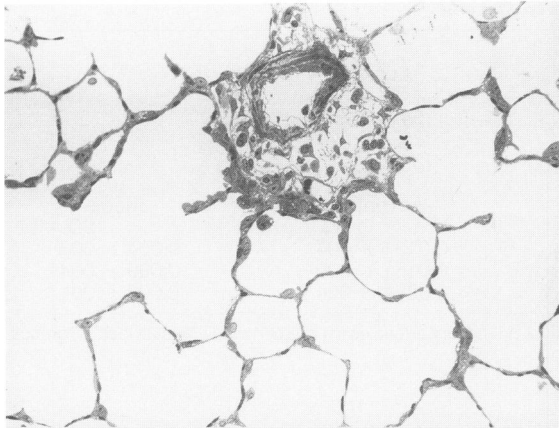


**Figure 9.** Light photomicrograph of lung from a rat 1 week PT with 3-MI. Vascular changes include perivascular edema and mononuclear inflammatory cell infiltration. Note mild type II epithelial cell hyperplasia is still evident. (Toluidine blue,  $\times 300$ .)

Target cell populations and degree of resistance to cytotoxic effects of 3-MI appear to vary among species. Type I epithelial cell necrosis is a consistent feature of 3-MI pneumotoxicity in ruminants<sup>3,7</sup> and mice<sup>9</sup> but not in the horse.<sup>12</sup> Pulmonary capillary endothelial cells have been shown to contain cytochrome P-450 mixed-function oxidases in the rabbit<sup>26</sup> and in the rat (C. G. Plopper, personal communication) that are required to metabolize 3-MI to an active electrophilic intermediate.<sup>2</sup> Type I epithelial cells are intimately associated with capillary endothelium and may be particularly sensitive to cytotoxicity because of their large membrane surface area and relative lack of organelles and endogenous detoxification mechanisms.

Our study is the first to demonstrate 3-MI-induced type I alveolar epithelial cell necrosis in the rat. Previous studies in rats either did not evaluate alveolar

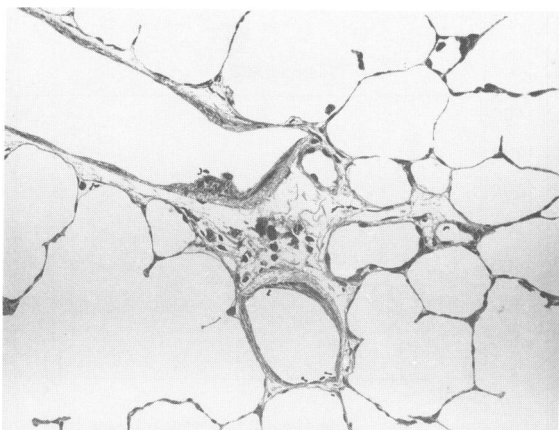


**Figure 10.** Light photomicrograph of lung from rat 2 weeks PT with 3-MI. Interstitial and perivascular mononuclear inflammatory cell clusters persist. Note epithelial changes have resolved. (Toluidine blue,  $\times 300$ .)

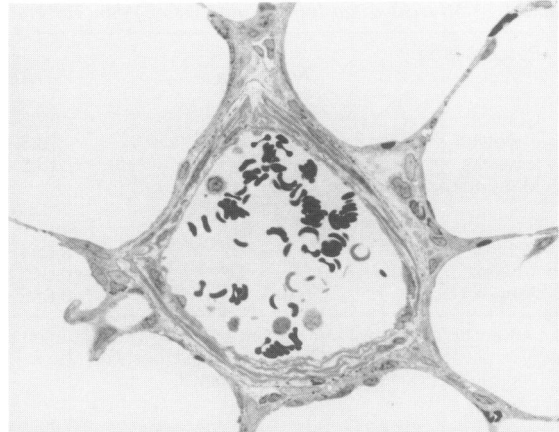


**Figure 11.** Light photomicrograph of an intraacinar arteriole with thickened tunica media and adventitia. (Toluidine blue,  $\times 900$ .)

epithelial cells<sup>13</sup> or terminated the study before the time point when epithelial changes were apparent, as found in our study.<sup>14</sup> In the former study, changes were evaluated by light microscopy, making differentiation of specific epithelial changes difficult. The type II cell hyperplasia seen in the former study may indicate that type I cell necrosis had occurred. It must also be noted that rats in the former study received dietary supplementation with vitamin E and selenium,<sup>13</sup> which may have mitigated epithelial changes. Selenium-containing enzymes of the glutathione peroxidase-glutathione reductase system have been shown to play an important role in detoxification of 3-MI. Pulmonary glutathione modulation has demonstrated that 3-MI-induced pneumotoxicity can be increased or decreased by depletion with diethyl maleate or supplementation with cysteine, respectively.<sup>27</sup>

3-Methylindole induces overt Clara cell necrosis in goats<sup>7</sup> and horses.<sup>12</sup> In horses, Clara cell necrosis is followed by degeneration and necrosis of the bronchiolar ciliated cells and results in chronic obstructive pulmonary disease.<sup>12</sup> Clara cell changes in the rats in this study were mild and characterized as autolysosome formation and persistent mucous cell "metaplasia." Mucus-secreting goblet cells are not normally present in the bronchioles of rats<sup>28</sup>; therefore, their presence 48 hours to 2 weeks PT is an indication of cellular transformation, most likely derived from the secretory Clara cell population. Transformation of airway surface epithelial serous to mucus cells as a result of airway irritation is well documented.<sup>29</sup> Clara cell pathology is a consistent feature of 3-MI pneumotoxicity in most species. This would correlate with the postulate that bioactivation of 3-MI is mediated by cytochrome P-450-dependent mixed-function oxidases, because high

**Table 1.** 3-MI-treated Rat Intra-acinar Vessel Mean Thickness and Area Percent\*

Percent area	Adventitia		Media		Lumen			
	Mean	SD	Mean	SD	Mean	SD		
Control	33.2	± 14.2	12.5	± 5.2	54.3	± 16.5		
1 week	41.8	± 11.3 <sup>†</sup>	18.5	± 6.9 <sup>†</sup>	39.7	± 11.1 <sup>†</sup>		
2 weeks	28.4	± 7.3	10.5	± 3.5	61.1	± 7.4		
Mean thickness (mm)	Vessel		Lumen		Adventitia		Media	
	Mean	SD	Mean	SD	Mean	SD	Mean	SD
Control	0.058	± .02	0.044	± .02	0.0101	± .004	0.004	± .003
1 week	0.065	± .02 <sup>†</sup>	0.040	± .01 <sup>†</sup>	0.0161	± .009 <sup>†</sup>	0.009	± .004 <sup>†</sup>
2 weeks	0.054	± .01	0.042	± .01	0.0084	± .004	0.003	± .001

\* Adventitial and medial area percent and mean thickness (mm) of intra-acinar pulmonary arterioles in control, 1 week, and 2 week PT groups (analysis of variance with Fischer's least-square post-hoc test,  $P < 0.05$ ).  
<sup>†</sup> Indicates significant elevation over control.

concentrations of smooth endoplasmic reticulum likely to contain cytochrome P-450 are present in Clara cells of rats, horses, and ruminants.<sup>30,31</sup> In our study, ciliated cells were also, yet less frequently, affected. Changes in ciliated cells are thought to be secondary to Clara cell injury, possibly because of loss of intercellular contact.<sup>12</sup>

Generalized endothelial cell necrosis was described 24 hours PT with 3-MI in a previous light microscopic study in rats,<sup>13</sup> but was not seen in our study or in a previous ultrastructural study 24 hours PT.<sup>14</sup> The difference in endothelial cell susceptibility may be related to the carrier agent used in the light microscopic study, and in fact, it was noted that control animals inoculated with Cremophore alone had mild, early vascular endothelial cell changes, which, in combination with 3-MI, may have initiated progressive injury.<sup>13</sup> Fixation technique and the difficulties in differentiating type I cells from endothelial cells by light microscopy also may explain these conflicting results. Endothelial cell changes have been reported in 3-MI-treated mice,<sup>9</sup> yet it was noted that neutrophils were present in capillary lumina in close

proximity to altered endothelial cells. These authors postulate that neutrophils could play a role in the development of 3-MI-induced endothelial cell damage. Focal endothelial cell necrosis was only seen rarely in our study 72 and 96 hours PT and was associated with focal aggregates of inflammatory cells, suggesting that endothelial cell injury is a non-specific change and probably a result of release of inflammatory mediators by local leukocytes.

Reports of microvascular endothelial cell injury are variable in different species. Early transient changes of endothelial cells and disruption of intercellular junctional integrity may be present in all species but missed in this study and others because of experimental design with respect to the time points studied. Perivascular edema is an early feature of 3-MI-induced toxicity in many species and may be an indication of altered endothelial permeability.<sup>7,9</sup> Plasma PGI<sub>2</sub> (measured as 6-keto-PGF<sub>1α</sub>) was significantly elevated before morphologic evidence of cell injury was apparent and may reflect early injury of endothelial cells because PGI<sub>2</sub> is an endothelial cell-derived prostaglandin. It should be remem-

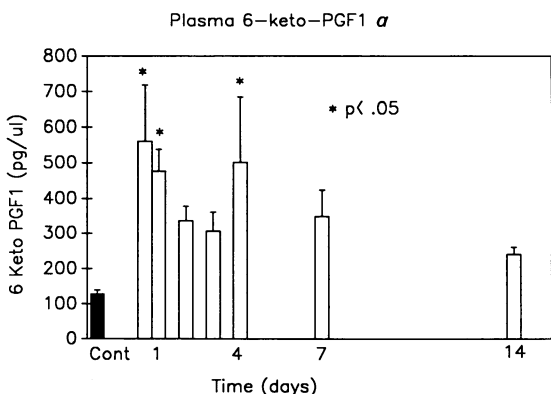


**Figure 12.** Plasma 6-keto-PGF<sub>1α</sub> concentrations in rats treated with 250 mg/kg 3-MI (nine treated and three control rats). \*indicates significant elevation over control (analysis of variance with Fischer's least significant difference post-hoc test,  $P < 0.05$ ).

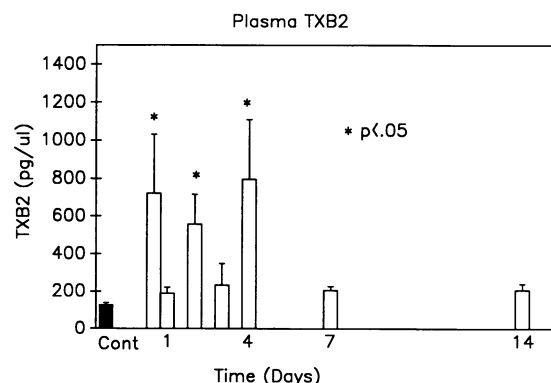


**Figure 13.** Plasma TxB<sub>2</sub> concentrations in rats treated with 250 mg/kg 3-MI (nine treated and three control rats). \*indicates significant elevation over control (analysis of variance with Fischer's least significant difference post-hoc test,  $P < 0.05$ ).



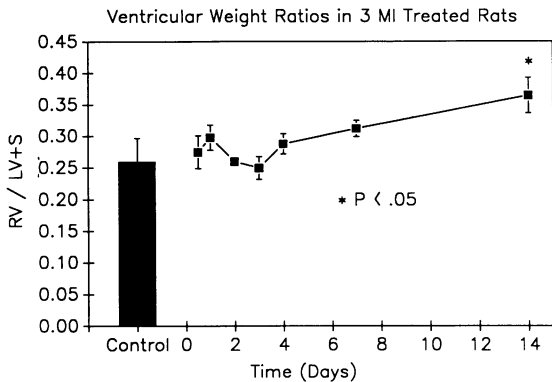


Figure 14. Ventricular weight ratios of rats treated with 250 mg/kg 3-MI. \*indicates significant elevation over control (analysis of variance with Fischer's least significant difference post-hoc test,  $P < 0.05$ ).

bered, however, that type II alveolar epithelial cells, alveolar macrophages, and lung fibroblasts also produce  $\text{PGI}_2$ .<sup>20-22</sup>

A previous study that examined plasma concentration of 6-keto- $\text{PGF}_{1\alpha}$  and  $\text{TxB}_2$  found no significant differences between controls and 3-MI-treated goats.<sup>32</sup> This work found radical fluctuations in concentrations of prostanoids in pretreated goats. We did not observe similar fluctuations in control values at variable time points in rats. In addition, significantly elevated concentrations of prostanoids in treated animals were 3 to 5 times the control values. Ruminants, in contrast to rats, have a significant population of intravascular macrophages that could contribute to the levels of circulating prostanoids.<sup>33</sup> The lack of significantly elevated plasma levels of prostanoids in goats may reflect more rapid metabolism and excretion of the acidic prostaglandin metabolites.

The second peak of plasma levels of 6-keto- $\text{PGF}_{1\alpha}$  96 hours PT corresponds to the peak proliferative stage when type II epithelial cells, alveolar macrophages, and lung fibroblasts show marked activity, and therefore may reflect prostaglandin production by these cells. In addition, inflammation was still prominent at this time point, and oxygen radicals evoked by the inflammatory process are known to stimulate synthesis of prostaglandins.<sup>34,35</sup>

$\text{TxA}_2$  (measured as  $\text{TxB}_2$ ) was elevated 12, 48, and 96 hours PT. Lung fibroblasts and platelets synthesize  $\text{TxA}_2$ , and neutrophils produce  $\text{TxA}_2$  during phagocytosis.<sup>18</sup> Although evidence of platelet aggregation was not apparent in our study, it has been noted to be a feature of 3-MI pneumotoxicity in some species.<sup>9</sup> Intravascular fixation may have removed platelet thrombi, or the inhibitory effects of  $\text{PGI}_2$  on platelet aggregation may have overcome the effects of  $\text{TxA}_2$ . Sustained levels at later time points

may reflect the fulminating inflammatory response and initiation of fibroplasia.

Repair of 3-MI-induced epithelial cell damage appears to be relatively complete by 2 weeks PT. Collagen levels, measured as hydroxyproline, were moderately increased over controls 1 and 2 weeks PT. This was apparent morphologically in the form of vascular medial fibrosis, which was most prominent at 1 week PT, and correlated with significant thickening of the vascular walls. Patchy fibrosis was also apparent at septal junctions in addition to mild, diffuse interstitial fibrosis, and may account for the higher collagen content of the lungs 2 weeks PT when morphologic evidence of perivascular thickening had subsided. Shifts in the ventricular weight ratios suggest the development of pulmonary hypertension in the 1 week and 2 week groups. Pulmonary hypertension may be associated with apparent transient smooth muscle hyperplasia, perivascular and interstitial deposition of extracellular matrix, or the vasoconstrictive effects of the circulating arachidonic acid metabolites ( $\text{TxA}_2$ ).

In conclusion, we have shown that 3-MI induces pulmonary injury in the rat with mild changes in Clara cells and necrosis of type I epithelial cells. Epithelial repair of 3-MI-induced injury in the rat appears to be relatively complete 2 weeks PT with residual mild septal fibrosis and pulmonary hypertension. We have also shown that inflammation may be intimately associated with the process of 3-MI injury of the lung. Finally, 3-MI-induced pneumotoxicity in the rat (at a dose of 250 mg/kg) is a good model of reversible epithelial cell injury and repair in the lung, and has potential as a model of pulmonary hypertension.

## References

1. Carlson JR, Dickinson EO, Yokoyama MT, Bradley BJ: Pulmonary edema and emphysema in cattle after intraruminal and intravenous administration of 3-methylindole. *Am J Vet Res* 1975, 36:1341-1347
2. Carlson JR, Yost GS: 3-Methylindole acute lung injury resulting from ruminal fermentation of tryptophan. In: Cheeke PR, ed. *Toxicants of Plant Origin*. Boca Raton, FL, CRC Press, 1989, Vol. 3, pp. 107-123
3. Atwal OS: Ultrastructural pathology of 3-methylindole-induced pneumotoxicity in cattle. *J Submicro Cytol* 1983, 15:433-445
4. Carlson JR, Yokoyama MT, Dickinson EO: Induction of pulmonary edema and emphysema in cattle and goats with 3-methylindole. *Science* 1972, 176:298-299
5. Bradley BJ, Carlson JR, Dickinson EO: 3-Methylindole-induced pulmonary edema and emphysema in sheep. *Am J Vet Res* 1978, 39:1355-1358

6. Huang TW, Carlson JR, Bray TM, Bradley BJ: 3-Methylindole-induced pulmonary injury in goats. *Am J Pathol* 1977, 87:647-666
7. Bradley BJ, Carlson JR: Ultrastructural pulmonary changes induced by intravenously administered 3-methylindole in goats. *Am J Pathol* 1980, 99:551-559
8. Turk MA, Flory W, Henk WG: Dose response in 3-methylindole-induced bronchiolar epithelial necrosis in mice. *Res Commun Chem Pathol Pharmacol* 1984, 46:351-362
9. Durham SK, Castleman WL: Pulmonary lesions induced by 3-methylindole in mice. *Am J Pathol* 1985, 121:128-137
10. Atwal OS, Persofsky MS: Ultrastructural pathology of intrapulmonary arteries in 3-methylindole-induced acute pulmonary edema and pulmonary arterial changes in cattle. *Am J Pathol* 1984, 114:472-486
11. Atwal OS, Persofsky MS: Ultrastructural pathology of intrapulmonary arteries in 3-methylindole-induced pneumotoxicity in cattle: II. Glycogen accumulation in the smooth muscle cells and intimal changes. *J Pathol* 1984, 142:141-149
12. Turk MA, Breeze RG, Gallina AM: Pathologic changes in 3-methylindole-induced equine bronchiolitis. *Am J Pathol* 1983, 110:209-217
13. Kiorpes AL, Keith IM, Dubielzig RR: Pulmonary changes in rats following administration of 3-methylindole in cremophore EL. *Histol Histopathol* 1988, 3:125-132
14. Adams JD, Laegreid WW, Huijzer JC, Hayman C, Yost GS: Pathology and glutathione status in 3-methylindole-treated rodents. *Res Commun Chem Pathol Pharmacol* 1988, 60:323-336
15. Derby-Dupont G, Radoux L, Haas M, Larbuisson R, Moel FX, Lamy M: Release of thromboxane B<sub>2</sub> during adult respiratory distress syndrome and its inhibition by nonsteroidal anti-inflammatory substances in man. *Arch Intern Pharmacodyn Ther* 1982, 259:317-319
16. Chandler DB, Giri SN: Changes in plasma concentrations of prostaglandins and plasma angiotensin-converting enzyme during bleomycin-induced lung fibrosis. *Am Rev Respir Dis* 1983, 128:71-76
17. Lemen RJ, Gates AJ, Mathe AA, Waring WW, Hyman AL, Kadowitz PJ: Relationship among digital clubbing disease severity and serum prostaglandins F<sub>2</sub> and E concentrations in cystic fibrosis patients. *Am Rev Respir Dis* 1978, 117:639-643
18. Slauson DO: The mediation of pulmonary inflammatory injury. *Adv Vet Sci Compar Med* 1982, 26:99-141
19. Hopkins NK, Sunn FF, Gorman RR: Thromboxane A<sub>2</sub> biosynthesis in human lung fibroblasts. *Biochem Biophys Res Commun* 1978, 85:827-836
20. Taylor L, Polgar P, MacAteer JA, Douglas WHJ: Prostaglandin production by type II alveolar epithelial cells. *Biochem Biophys Acta* 1979, 572:502-509
21. Hsueh W: Prostaglandin biosynthesis in pulmonary macrophages. *Am J Pathol* 1979, 97:137-148
22. Splawinski J, Fryglewski RJ: Release of prostacyclin by the lung. *Bull Eur Physiopathol Respir* 1981, 17:553-569
23. Nowell JA, Pangborn J, Tyler WS: Stabilization and replication of soft tubular and alveolar systems. A scanning electron microscope study of the lungs, In: Johari O, Cowin I, eds. *Scanning Electron Microscopy*. Chicago, IIT Research Institute, 1972, pp. 305-313
24. Wilson DW, Segall HJ, Pan LCW, et al: Progressive inflammatory and structural changes in the pulmonary vasculature of monocrotaline-treated rats. *Microvasc Res* 1989, 38:57-80
25. Woessner JF: The determination of hydroxyproline in tissue and protein samples containing small proportions of this amino acid. *Arch Biochem Biophys* 1961, 93:440-447
26. Serabjit-Singh, Nishio CJSJ, Philpot RM, Plopper CG: The distribution of cytochrome P-450 monooxygenase in cells of rabbit lung: An ultrastructural immunocytochemical characterization. *Mol Pharmacol* 33:279-289
27. Nocerini MR, Carlson JR, Breeze RG: Effect of glutathione status on covalent binding and pneumotoxicity of 3-methylindole in goats. *Life Sci* 1983, 32:449-458
28. Mawdesley-Thomas LE, Healey P, Barry DH: Experimental bronchitis in animals due to sulphur dioxide and cigarette smoke. An automated quantitative study. In: Walton WH, ed. *Proceedings of an International Symposium on Inhaled Particles*. London, Unwin Bros, 1971, pp. 509-525
29. Jeffery PK: Goblet cell increase in rat bronchial epithelium arising from irritation or drug administration—an experimental and electron microscopic study. PhD Thesis. University of London, 1973
30. Jones K, Holland J, Foureman G, Band J, Fouts J: Induction of xenobiotic metabolism in Clara cells and alveolar type II cells isolated from rat lungs. *J Pharmacol Exp Ther* 1983, 225:316-319
31. Plopper CG, Dungworth DL: Structure, function, cell injury and cell renewal of bronchiolar and alveolar epithelium. In: McDowell E, ed. *Lung Carcinomas*. New York, Churchill Livingstone, 1987, pp. 94-128
32. Acton KS, Bray TM, Boermans HJ: Effect of 3-methylindole on the plasma and lung concentrations of prostaglandins and thromboxane B<sub>2</sub> in goats. *Comp Biochem Physiol* 1989, 94A:677-681
33. Warner AE, Barry BE, Brain JD: Pulmonary intravascular macrophages in sheep—Morphology and function of a novel constituent of the mononuclear phagocyte system. *Lab Invest* 1986, 55:276-288
34. Panganamala RV, Brownlee NR, Sprechen H, Cronwell DB: Evaluation of superoxide anion and singlet oxygen in the biosynthesis of prostaglandins from eicosa 8,11,14-trienoic acid. *Prostaglandins* 1974, 7:21-28
35. Rahimtula A, O'Brien PJ: The possible involvement of singlet oxygen in prostaglandin biosynthesis. *Biochem Biophys Res Commun* 1976, 70:893-899